JETIR.ORG ISSN: 2349-5162 | ESTD Year : 2014 | Monthly Issue
JOURNAL OF EMERGING TECHNOLOGIES AND INNOVATIVE RESEARCH (JETIR)
An International Scholarly Open Access, Peer-reviewed, Refereed Journal

MICs synthesized by the SEPIC-type PCSC with different prime converters with buck-boost converter

[1] Manoj Kumar Singh, [2] Abhishek Kumar Singh, [3] Gaurav, [4] Vijay Kumar Tewari

[1]Student, [2]Student, [3]Student, [4]Assistant Professor
[1] Department of Electrical Engineering,
[1] Rajkiya Engineering College
Kannauj, India

Abstract :

In this research, in order to compare and contrast several prime converters, including the Buck-Boost Converter, that are integrated into the SEPIC-type PCSC architecture in order to synthesize Multiple-Input Converters (MICs). Under different operating situations, the research examines the MICs' performance parameters, including efficiency, voltage regulation, and transient responses. The effectiveness of using various prime converters with the SEPIC- type PCSC for MIC synthesis is investigated in detail through simulation and experimental validation. The results contribute to our knowledge and understanding of multi-input power conversion systems by clearing the concept on how to choose prime converters for different types of applications. "Charging and discharging the ESS efficiently and maximizing power extraction from the solar panels are both made possible by the converter's buck-boost characteristic. Depending on the ESS's charging status, three distinct modes of operation are described. The proposed converter's steady-state and dynamic behavior are examined thoroughly. In order to back up the analysis and the feasibility of the proposed converter, experimental results are provided.

Keywords **- SEPIC Converter, Buck-Boost Converter, RGA Theory, MIC's**

.

I. INTRODUCTION

These days, renewable energy sources such as wind and photovoltaic (PV) systems are receiving a lot of attention. These energy sources' main drawback is their irregularity, which prevents "the continuous delivery of power." Therefore, other supplemental natural resources and their capacity to supply constant electricity. Fuel cells (FC) and batteries, two further forms of alternative energy, are thus required [1]-[2]. For these hybridized systems to effectively manage the power from multiple sources, multi-input converters (MICs) are crucial. The efficiency, size, cost, and performance of MICs are superior to those of several separate converters. MICS reduce complexity and system costs while providing a simpler, more compact design [3]-[6].

To assess MICs, one must adhere to the requirements, limits, and assumptions stated. As stated in, a generic approach to MIC creation is proposed. Based on research into converter topologies, the synthesis technique (MICs) involves connecting an additional pulse voltage or current source to a converter [7]. The three potential topologies for the multi-input DC/DC converter suggested in the paper are depicted in Figure 1. In order to lower costs and improve system efficiency, it will recommend an updated flyback-forward topology-based three-port DC/DC converter for freestanding PV systems. Combined grid applications include street lighting and powering loads coupled to multi-input buck and boost converters. The multi-input boost-type converter described in integrates a bidirectional storage element port with two unidirectional input power ports into a single, cohesive construction [6]. In this design, there are only two power switches, and each of them has two duty cycles of its own. The capacity to increase action is a unique characteristic of the proposed converter and is especially useful for dc grid applications [11]. However, the interplay between the control structure and itself is the determining factor in choosing the storage element for a unified system. The proposed structure makes use of a total of two power switches, with two duty cycles per switch. Using multiple inputs and outputs (MIMO), a non-isolated DC/DC buck-boost converter is proposed . Any combination of input sources can be used to distribute the load power in the converter. In, this suggested MIC that uses a z-source converter as its foundation; however, the number of capacitors and inductors used is identical to that of a z-source converter with a single input [13]. Both the system's reliability and the utilization of renewable sources are improved by MICs. Here is the MIC block diagram: A few of the benefits of MICs are: 1) MICs keep the supply flowing, which makes the system more dependable, 2) With the use of MICs, a common load can be generated from multiple sources. 3) MICs overcome other converters in terms of efficiency, 4) The load can be powered by each source separately or all at once [14]. A single-load, double-input converter is the focus on the project. The micro-grid, energy storage systems, automobile, aircraft, and satellite sectors are some of the many uses for MICs (Double Input)

[17]. PSCs, or pulsing source cells, are a part of MICs. The two most popular forms of pulsing source cells used in the manufacturing of MICs are pulsating voltage source cells and pulsating current source cells [16].

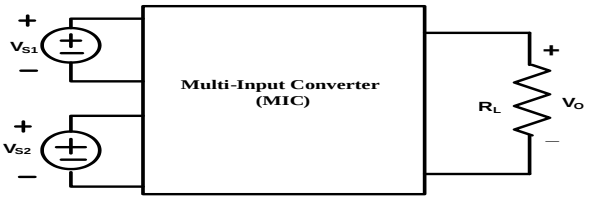

Fig. 1. Multi-Input Converter (MIC)

1.1 BRIEF REVIEW OF BASIC PWM CONVERTER TOPOLOGIES

Power electronics often make use of six basic PWM converters: buck, boost, buck-boost, Cuk, zeta, and single- ended primary inductance converter (SEPIC). There are often two or three distinct parts to a simple pulse width modulation (PWM) converter: the input (IP), the energy buffer (EBP), and the output (OP). There are no energy buffer in a buck or boost converter included in the topological diagrams of the six most fundamental PWM converters are their input sections, energy buffer sections, and output portions, energy storage systems, the automotive, aerospace and output portions marked. There has been an energy buffer section when the inductor and capacitor are used. In Figure 2, the inductors and capacitors in the input section store energy throughout a switching cycle. Then, without losing any energy, the stored energy is transferred to the output section.

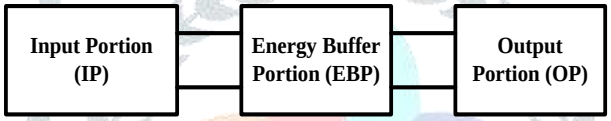

Fig .2 . Three portions of a basic PWM converter

During the operation, each inductor has a non-zero direct current flowing through it, and each capacitor has a non- zero direct current voltage across it. An inductor might be seen as a current buffer, while a capacitor might be seen as a voltage buffer. To make the PWM converter topologies easier to understand, Fig. 3 uses rectangular components to represent the voltage buffer or the current buffer.The DC-to-DC converter, SEPIC Converter credibly maintain an output voltage that is less than, equal to, or greater than the input voltage, as shown in Fig. 5. To get the output of a SEPIC Converter, there must have to pay attention at its duty cycle. Fig. 3 shows that a SEPIC converter's most important characteristics are its buck, boost, and buck-boost converter capabilities.

The SEPIC converter contains inductors and capacitor that plays a important role from converters, the voltage of one magnitude to another. SEPIC Converter is better than other converters in terms of efficiency and input current capabilities. It has low switching loss and little overshot.

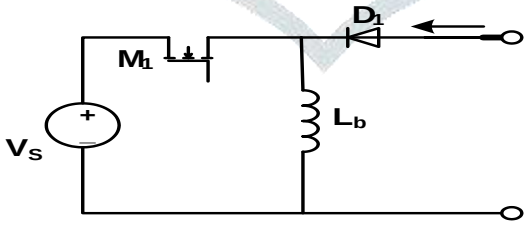

Fig. 4. Buck- Boost PCSC

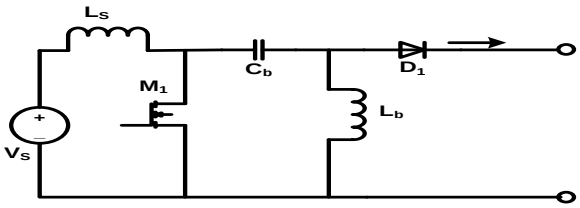

Fig. 5. SEPIC -type PCSC

1.2 GENERATION OF MICS WITH PCSCS

The following stages can also be used to outline the synthesis process of the MICs using PCSC.

Step 1: Choose one of the PCSCs shown in Fig.5
Step 2: In order to need a PWM converter with voltage buffers or a voltage sink, choose one of the six basic models.
Step 3: After deciding on a prime PWM converter and PCSC, follow rules 1 and 2 to insert them.
Step 4: Before inserting the PCSC, make sure it follows rule 3. Afterwards, the MIC's final version can be acquired.

II. MODELLING AND ANALYSIS OF INTEGRATED SEPIC (PCSC)-BUCK BOOST CONVERTER

The proposed SEPIC (PCSC) Buck Boost converter is a parallel combination of SEPIC (PCSC) with Buck Boost converter. Fig. 6 is circuit of SEPIC (PCSC) - Boost Converter:

The circuit can operate in continuous or discontinuous inductor mode. The two-input SEPIC-Buck Boost converter for DC-DC conversion which distributes the power through decoupled single-loops on for DC voltage DC source current regulation. (Fig 6).

Table 2.1: Operation of switch and diode

Device	Mode-1	Mode-2	Mode-3
Switch S_1	ON	OFF	OFF
Switch S_2	ON	ON	OFF
Diode D_1	OFF	ON	ON
Diode D_2	OFF	OFF	ON

Splitting the whole load demand between Vg_1 and Vg_2 is the converter's intended function. By utilizing the high voltage or primary source to provide the surplus load, the converter allows the Low Voltage Source (LVS) to operate at its maximum capacity. The SEPIC-Buck Boost converter relies on the duty ratio to function.

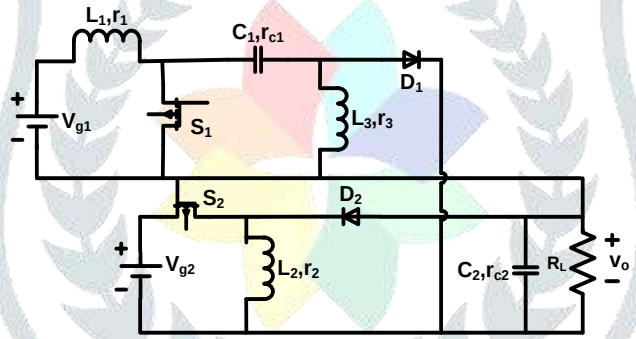

Fig. 6. SEPIC Buck Boost Converter

The two-input SEPIC (PCSC) - Buck Boost converter operates in 3 different modes during a single switching cycle.

A. Analysis of Mode 1 :(0 < t <d_1T_s)

During mode 1, switches S_1 and S_2 are activated while diodes D_1 and D_2 are deactivated as shown in Table 2.1. Inductors L_1 and L_2 are charging linearly from dc sources Vg_1 and Vg_2, while capacitor C_1 is charging inductor L_3 linearly. Capacitor C_2 stabilizes the load voltage. Fig. 7 illustrates the switching pattern of this mode.

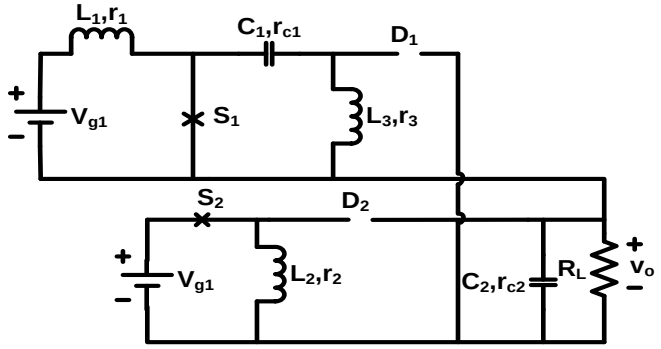

Fig. 7. Equivalent diagram of Mode-1

State space matrix of mode 1 is :-

$$A1 = \begin{bmatrix} -\frac{r_1}{L_1} & 0 & 0 & 0 & 0 \\ 0 & -r_2/L_2 & 0 & 0 & 0 \\ 0 & 0 & -(r_{C1}+r_3)/L_3 & -1/L_3 & 0 \\ 0 & 0 & 1/C_1 & 0 & 0 \\ 0 & 0 & 0 & 0 & -\frac{1}{C_2(R_L+r_{C2})} \end{bmatrix} \quad (1)$$

The expression for mode-1's input matrix B_1 is as follows:

$$B_2 = \begin{bmatrix} \frac{1}{L_1} & 0 \\ 0 & \frac{1}{L_2} \\ 0 & 0 \\ 0 & 0 \\ 0 & 0 \end{bmatrix} \quad (2)$$

Input current matrix P_1 for mode-1 is:-

$$P_1 = \begin{bmatrix} 1 & 0 & 0 & 0 & 0 \\ 0 & 1 & 0 & 0 & 0 \end{bmatrix} \quad (3)$$

Output matrix E_1 can be expressed as:-

$$E_1 = \begin{bmatrix} 0 & 0 & 0 & 0 & \frac{R_L}{r_{C2}+R_L} \end{bmatrix} \quad (4)$$

Feed through matrix F_1 for mode -1 is expressed as:-

$$F_1 = [0] \quad (5)$$

B. Analysis of Mode-2: ($d_1T_S<t<T_S(d_2-d_1)$)

During mode-2, switch S_1 is deactivated while switch S_2, which is the sepic converter switch, is activated. Diode D_1 is activated while diode D_2 is deactivated according to Table 1, Inductor L_1 current falls linearly, while inductor L_2 current increases linearly. In this configuration, the SEPIC converter's buffer capacitor C_1 receives the energy from the buck-boost converter's inductor. The transition pattern of this mode is seen in Fig.8

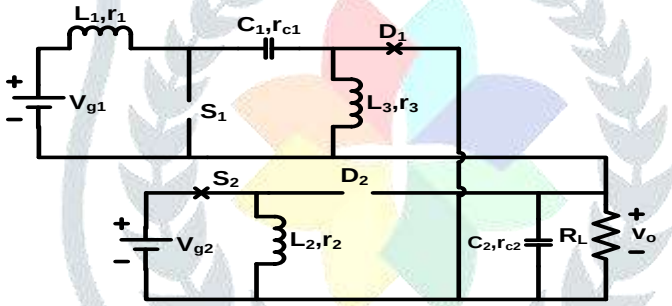

Fig. 8. Equivalent diagram of Mode-2

State space matrix of mode-2:-

$$A_2 = \begin{bmatrix} -\frac{1}{L_1}\left(r_1 + r_{C1} + \frac{R_L r_{C2}}{r_L + r_{C2}}\right) & 0 & -\frac{1}{L_1} & -\frac{1}{L_1}\left(\frac{R_L}{R_L + r_{C2}}\right)\frac{1}{L_1} \\ 0 & \frac{(-r_2)}{L_2} & 0 & 0 & 0 \\ \frac{1}{L_3}\left(\frac{R_L r_{C2}}{R_L + r_{C2}}\right) & 0 & \left(r_3 + \frac{R_L r_{C2}}{(R_L + r_{C2})}\right)\frac{1}{L_3} & 0 & \left(\frac{-R_L}{R_L + r_{C2}}\right)\frac{1}{L_3} \\ \frac{1}{C_1} & 0 & 0 & 0 & 0 \\ \frac{-R_L}{C_2(R_L + r_{C2})} & 0 & \frac{R_L}{C_2(R_L + r_{C2})} & 0 & \frac{-1}{C_2(R_L + r_{C2})} \end{bmatrix} \quad (6)$$

The expression for mode-1's input matrix B_2 is as follows:

$$B_2 = \begin{bmatrix} \frac{1}{L_1} & 0 \\ 0 & \frac{1}{L_2} \\ 0 & 0 \\ 0 & 0 \\ 0 & 0 \end{bmatrix} \quad (7)$$

Input current matrix P_2 for mode-2 is:-

$$P_2 = \begin{bmatrix} 1 & 0 & 0 & 0 & 0 \\ 0 & 1 & 0 & 0 & 0 \end{bmatrix} \quad (8)$$

Output matrix E_2 can be expressed as:-

$$E_2 = \begin{bmatrix} \frac{-R_L r_{C2}}{r_{C2}+R_L} & 0 & \frac{R_L r_{C2}}{r_{C2}+R_L} & 0 & \frac{R_L}{r_{C2}+R_L} \end{bmatrix} \quad (9)$$

Feed through matrix F_1 for mode -2 is expressed as:-

$$F_2 = [0] \quad (10)$$

C. Analysis of Mode-3: (Ts (d_2-d_1) <t<Ts)

For mode-3, see Table 1 for the configuration that turns off all switches (S_1, S_2) and turns on both diodes (D_1, D_2), As illustrated in Figure 9, this mode permits simultaneous power delivery to the load from both dc-sources.

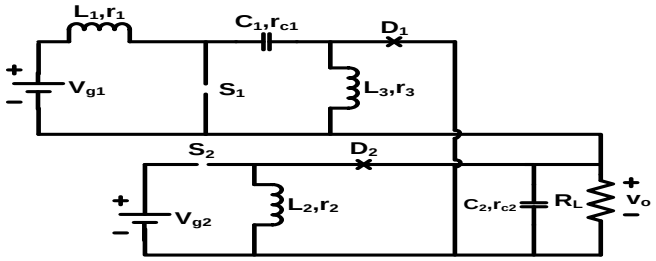

Fig. 9. Equivalent diagram of Mode-3

State space matrix of mode-3:-

$$A3 = \begin{bmatrix} -\frac{1}{L_1}\left(r_1 + r_{C1} + \frac{R_L r_{C2}}{r_L + r_{C2}}\right) & \left(\frac{-R_L r_{C2}}{R_L + r_{C2}}\right)\frac{1}{(L_1)} & \left(\frac{R_L r_{C2}}{R_L + r_{C2}}\right)\frac{1}{(L_1)} & -\frac{1}{L_1} & \left(\frac{R_L}{R_L + r_{C2}}\right)\frac{1}{L_1} \\ -\frac{1}{L_2}\left(\frac{R_L r_{C2}}{R_L + r_{C2}}\right) & -\left(r_2 + \frac{R_L r_{C2}}{(R_L + r_{C2})}\right)\frac{1}{(L_2)} & \left(\frac{R_L r_{C2}}{R_L + r_{C2}}\right)\frac{1}{L_2} & 0 & \left(\frac{R_L}{R_L + r_{C2}}\right)\frac{1}{L_2} \\ \frac{1}{(L_3)}\left(\frac{R_L r_{C2}}{R_L + r_{C2}}\right) & \frac{1}{(L_3)}\left(\frac{R_L r_{C2}}{R_L + r_{C2}}\right) & -\left(r_3 + \frac{R_L r_{C2}}{R_L + r_{C2}}\right)\frac{1}{L_3} & 0 & \left(\frac{-R_L}{R_L + r_{C2}}\right)\frac{1}{L_3} \\ \frac{1}{C_1} & 0 & 0 & 0 & 0 \\ \frac{-R_L}{(C_2)(R_L + r_{C2})} & \frac{-R_L}{C_2(R_L + r_{C2})} & \frac{R_L}{C_2(R_L + r_{C2})} & 0 & \frac{-1}{C_2(R_L + r_{C2})} \end{bmatrix} \quad (11)$$

The expression for mode-3's input matrix B_3 is as follows:

$$B_3 = \begin{bmatrix} \frac{1}{L_1} & 0 \\ 0 & 0 \\ 0 & 0 \\ 0 & 0 \\ 0 & 0 \end{bmatrix} \quad (12)$$

Input current matrix P_3 for mode-3 is:-

$$P_3 = \begin{bmatrix} 1 & 0 & 0 & 0 & 0 \\ 0 & 1 & 0 & 0 & 0 \end{bmatrix} \quad (13)$$

Output matrix E_3 can be expressed as:-

$$E_3 = \left[\frac{-R_L r_{C2}}{r_{C2}+R_L} \quad \frac{-R_L r_{C2}}{r_{C2}+R_L} \quad \frac{R_L r_{C2}}{r_{C2}+R_L} \quad 0 \quad \frac{R_L}{r_{C2}+R_L}\right] \quad (14)$$

Feed through matrix F_3 for mode -3 is expressed as:-

$$F_3 = [0] \quad (15)$$

III. VOLTAGE CONVERSION RATIO OF MIC

By using the volt-sec balance concept to all of the inductors connected to the converter, in order to determine its voltage conversion ratio. Throughout a switching cycle, the voltage across all inductors is calculated in each mode.

For inductor-L1

$V_{g1}d_1+(V_{g1}+V_{C2}-V_{C1})(d_2-d_1)+(V_{g1}+V_{C2}-V_{C1})(1-d_2) = 0$ (16)

For inductor-L2

$V_{g2}d_1+V_{g2}(d_2-d_1)+V_{C2}(1-d_2) = 0$ (17)

For inductor-L3;

$-V_{C1}d_1 - V_O(d_2-d_1) - V_O(1-d_2) = 0$ (18)

Solving above eq(16), (17), (18) we get value of V_O;

$$\mathbf{V_O} = \left[\frac{\boldsymbol{V_{g1}}}{(\mathbf{1}-\boldsymbol{d_1})} - \frac{\boldsymbol{V_{g2}d_2}}{(\mathbf{1}-\boldsymbol{d_2})}\right] \quad (19)$$

The value of the output voltage consist of two major term and directly depends on the input voltages Vg_1,Vg_2 and duty ratio d_1,d_2 of the two MOSFET switches". Equation (19) gives the formula for the load voltage. It is clear from this equation that the converter is providing boosting action with regard to source 1, and with respect to source2.Once again, the converter is simulating bucking. The magnitude of the input dc sources and the duty ratio of both switches determine the voltage gain expression of the MIC, as shown in Eq. (19). Therefore, the suggested converter is buck- boost active independent of the two dc inputs.

IV. CONVERTER PECIFICATIONS

For designing the converter in open loop simulation, there should be a specified value of the use parameters. The respective value of each parameter is mentioned below:

Table 4.1 : Converter specification

Design parameter	Expression	Value of Parameters
L_1	$\frac{V_{g1} * d_1}{f_s * (\Delta i_{L1})}$	500 µH
L_2	$\frac{V_{g2} * d_1}{f_s * \Delta i_{L2}}$	312 µH
L_3	$\frac{v_0 * (1 - d_1)}{f_s * (\Delta i_{L3})}$	100 µH
C_1	$\frac{i_{L3} * d_1}{f_s * (\Delta v_{c1})}$	27 µF
C_2	$\frac{i_0 * d_1}{f_s * (\Delta v_{c2})}$	60 µF

Table 4.2 : Design expression and parameter valve

Parameters	Numerical Value
Power rating	P ≈ 177 W
DC Load voltage	V_O = 48 V
DC source voltage	V_{g1}=36 V, V_{g2}=24 V
Ripple current	≤ 10%
Ripple voltage	≤ 5%
Switching frequency	50 kHz

V. DISCRETE-TIME MODELLING OR MIC

As far as simulations of switching power converters proceed, discrete-time modeling (DTM) stands out. A MIC's constant performance at a fixed switching frequency might be described using the DTM. It is simple to implement the digital compensator design in MATLAB after the discrete-time model is supplied. The technique computes the system dynamics quickly and consistently, making it an excellent for modelling the periodic behaviour of MICs with constant-frequency switching. It will enable to create a discrete-time compensator and increase the accuracy of the model.The digital compensator design may be executed with ease, if the discrete- time model is made available. Two distinct pulse width modulation (PWM) techniques, trailing-edge modulation and leading-edge modulation, are commonly employed in switch mode DC-DC converters.

In one switching cycle, dc-dc converters can operate in two or more modes, and their non-linear circuits are well-known. But since the circuit is linearly time invariant across all modes of operation, the state equation can be used to describe its behavior in the k^{th} mode of operation, given by

$$t_k \in [kT_s, (n+k)T_s] \begin{cases} \dot{x} = A_k x + b_k u \\ y = E_k x + F_k u \end{cases}$$

Where $A \in R^{N\times N}, B_K \in R^{N\times 1}, E_K \in R^{1\times N}, and\ F \in R, 'x$ "u" represents the excitation vector and 'y' represents the output vector; such vector often indicates the number of energy storage elements, including inductor currents and capacitor voltages, and it has 'N' states. Using the state-space averaging method is one approach to obtaining the state equation:

$$[\dot{X}] = [(A_1 - A_2)d_1 + (A_2 - A_3)d_2 + A_3][X]$$
$$+[(B_1 - B_2)d_1 + (B_2 - B_3)d_2 + B_3][U] \quad (20)$$

Including perturbations and simplifying for the small-signal model given by:

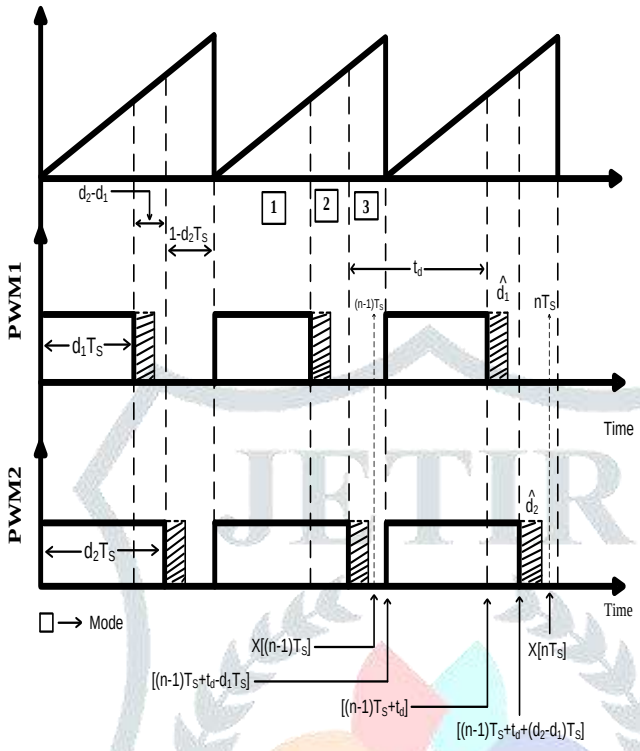

Fig. 10. Waveforms for trailing – edge OFF-Time sampling

$$\dot{X}+\hat{x}=\left[(A_1-A_2)(d_1+\widehat{d_1})+(A_2-A_3)(d_2+\widehat{d_2})+A_3\right][X+\hat{x}]+\left[(B_1-B_2)(d_1+\widehat{d_1})+(B_2-B_3)(d_2+\widehat{d_2})+B_3\right][U]$$

$$\hat{x}=A\hat{x}+B\hat{u}+k_1\,\hat{d}+k_2\,\hat{d} \qquad (21)$$

where $k_1=[(A_1-A_2)X+(B_1-B_2)U]$ $k_2=[(A_2-A_3)X+(B_2-B_3)U]$.

The change in the duty ratio is represented as an impulse function:

$$\hat{d}=\sum_{-\infty}^{\infty}(n-1)T_s\delta[t-\left((n-1)T_s+t_d\right)]$$

In trailing-edge modulation, the pulse width modulation (PWM) signal is turned on at the beginning of the clock signal and turned off at the intersection of the error signal and the ramp waveform. The term "trailing-edge OFF-time modulation" describes a method of signal sampling that occurs at the exact moment when both switches are turned off. There is a one- period analysis that begins at the sampling instant and continues for nTs, following a sample interval of (n-1)Ts.

Interval 1: $(n-1)T_s<t<[(n-1)T_s+t_d-d_1T_s]$
There is no variation in duty ratios throughout this time:
$\widehat{d_1}=0,\ \widehat{d_2}=0,\ \hat{u}=0$
Output of 1^{st} *interval* after solving equation is

$$\hat{x}[(n-1)T_s+t_d-d_1T_s]=e^{A_3(t_d-d_1T_s)}.\hat{x}[(n-1)T_s] \qquad (22)$$

Interval -2: $[(n-1)T_s+t_d-d_1T_s]<t<[(n-1)T_s+t_d]$
In this interval, there is no change or perturbation in duty ratios, therefore
$\hat{d}_1=0,\ \widehat{d_2}=0,\ \hat{u}=0$
Output of 2^{nd} interval after solving equation is

$$\hat{x}[(n-1)T_s+t_d]=e^{A_1d_1T_s}*e^{A_3(t_d-d_1T_s)}*\hat{x}[(n-1)T_s] \qquad (23)$$

Interval -3: $[(n-1)T_s+t_d]<t<[(n-1)T_s+t_d+(d_2-d_1)T_s]$
During this interval there is a possibility to have variations in duty ratio and therefore
$\hat{d}_1\neq 0,\ \widehat{d_2}=0,\ \hat{u}=0$
Output of 3^{rd} interval after solving equation

$$\hat{x}[(n-1)T_s+t_d+(d_2-d_1)T_s]=e^{A_1d_1T_s}e^{A_3(t_d-d_1T_s)}e^{A_2(d_2-d_1)T_s}\hat{x}[(n-1)T_s]+k_1T_s\widehat{d_1}(n-1)e^{A_2(d_2-d_1)T_s} \qquad (24)$$

Interval -4: $[(n-1)T_s+t_d+(d_2-d_1)T_s]<t<[nT_s]$
During this phase, there is a chance of fluctuations in duty ratios, and therefore

$$\hat{d}_2\neq 0, \qquad \widehat{d_1}=0, \qquad \hat{u}=0$$

Output of 4^{th} interval after solving equation

$$\varphi = e^{AT_s}$$

$$\gamma_1 = k_1 T_s e^{[A_1(d_2-d_1)T_s + A_2(T_s - t_d - d_1 T_s)]}$$

$$\gamma_2 = k_2 T_s e^{A_3[T_s - t_d - d_2 T_s + d_1 T_s]} \quad (25)$$

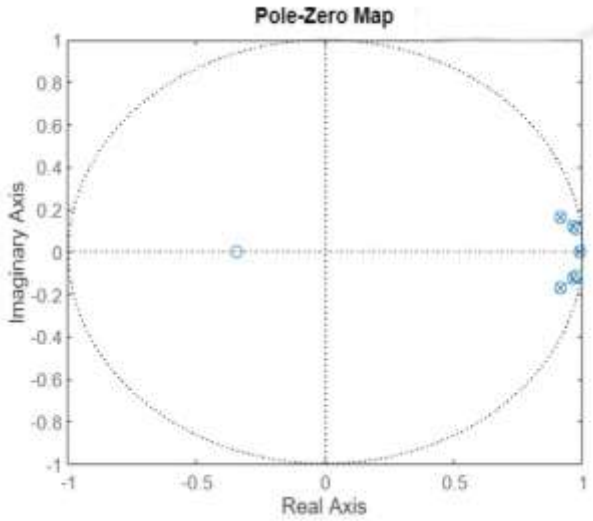

Fig. 11. Pole –zero diagram

A pole-zero plot shows the location in the complex plane of the poles and zeros of the transfer function of a dynamic system, such as a controller, compensator, sensor, equalizer, filter, or communications channel.The stability study of the converter can be completed after the transfer function of the plot and controller are determined (Fig.11.). displays the converter's pole-zero map, where every pole and zero is located inside a unit circle, producing a stable closed-loop structure.

VI. RESULTS

In the paper, the accuracy of the discrete-time models created for multi-state converters is verified through experimental and computational analysis of a two-input buck-boost dc-dc converter." By observing the converter's open-loop performance, it might deduce that the load requirement is satisfied even when source- 2 is disconnected from the load. By source-1 with a load current of 3.67 A. At 48 volts, the load voltage become constant.

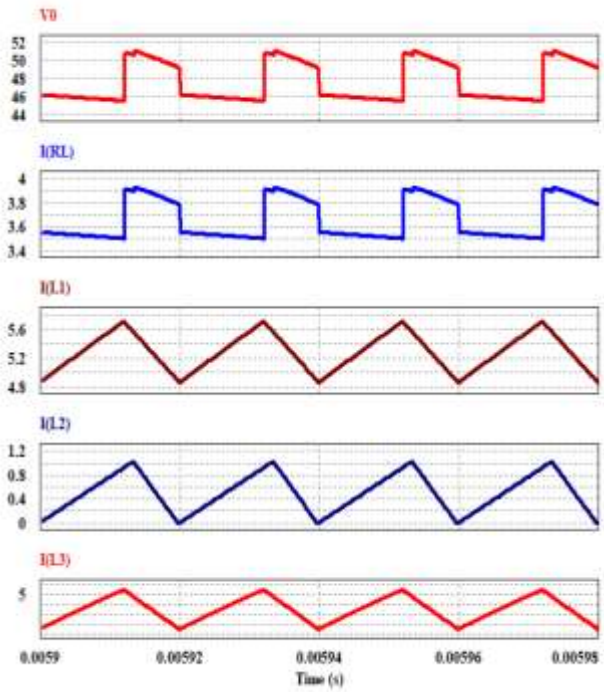

VII. CONCLUSION

The attention to MIC's synthesis using the Pulse Controlled Switching Converter (PCSC) and the SEPIC Buck Boost topology in this paper. Our analysis of the merits, demerits, and potential uses of this method is comprehensive. It began by conducting extensive testing and evaluations to demonstrate that the proposed converter could effectively synthesis microphone signals with higher quality and reduced noise. By integrating the SEPIC Buck Boost design with PCSC control mechanisms, though it might be able to precisely regulate voltage and current, resulting in significantly improved signal quality compared to traditional synthesis methods. By comparing it to other converter topologies, it might be able to prove that the SEPIC Buck Boost MIC's Synthesized PCSC Converter was effective, flexible, and plastic. The converter is a versatile choice for many MIC's synthesis tasks due to its ability to seamlessly transition between boost and buck modes without performance degradation.

In conclusion, in order to clear the concept on critical new questions regarding the design, implementation, and evaluation of MIC's synthesis systems based on PCSC control and the SEPIC Buck Boost topology. The proposed converter has several potential applications in numerous domains, such as audio processing and telecommunications, thanks to its improved signal quality, efficiency, and adaptability.

REFERENCES

[1] Y. -C. Liu and Y. -M. Chen, "A Systematic Approach to Synthesizing Multi-Input DC–DC Converters," in IEEE Transactions on Power Electronics, vol. 24, no. 1, pp. 116-127, Jan. 2009, doi: 10.1109/TPEL.2008.2009170.

[2] M. Shen, F. Z. Peng, and L. M. Tolbert, "Multilevel DC–DC power conversion system with multiple DC sources," IEEE Trans. Power Electron.vol. 23, no. 1, pp. 420–426, Jan. 2008.

[3] B. G. Dobbs and P. L. Chapman, "A multiple-input DC-DC converter topology," IEEE Power Electron. Letters, vol. 1, pp. 6–9, Mar. 2003.

[4] Saeideh Khadem Haghighian, Sajjad Tohidi, Mohammad Reza Feyzi, Mehran Sabahi "Design, and analysis of a novel SEPIC-based multi-input DC/DC converter" IET Power Electron., Vol. 4, pp. 1393-1402, 2017.

[5] Reza Moradpour, Hossein Ardi, "Design and implementation of a New SEPIC –Based High Step-Up DC/DC Converter for Renewable Energy Applications" IEEE Trans. Power electronics 10.1109/TIE.2017.2733421.

[6] H.-J. Chiu, H.-M. Huang, L.-W. Lin, and M.-H. Tseng, "A multiple-input DC/DC converter for renewable energy systems," in Proc. IEEE ICIT 2005, pp. 1304–1308

[7] Y.-M. Chen, Y.-C. Liu, and S.-H. Lin, "Double input PWM DC/DC converter for high-/low-voltage sources," IEEE Trans. Ind. Electron., vol. 53, no. 5, pp. 1538–1545, Oct. 2006.

[8] H. Matsuo, K. Kobayashi, Y. Sekine, M. Asano, and L. Wenzhong, "Novel solar cell power supply system using the multiple-input DC–DC converter," in Proc. IEEE INTELEC 1998, pp. 797–802.

[9] K. Kobayashi, H. Matsuo, and Y. Sekine, "Novel solar-cell power supply system using a multiple-input DC–DC converter," IEEE Trans. Ind.Electron., vol. 53, no. 1, pp. 281–286, Feb. 2006.

[10] A. Di Napoli, F. Crescimbini, S. Rodo, and L. Solero, "Multiple input DC–DC power converter for fuel-cell powered hybrid vehicles," in Proc.IEEE Power Electron. Spec. Conf. 2002, pp. 1685–1690.

[11] L. Solero, A. Lidozzi, and J. A. Pomilio, "Design of multiple-input power converter for hybrid vehicles," IEEE Trans. Power Electron., vol. 20,no. 5, pp. 1007–1016, Sep. 2005.

[12] F. Blaabjerg, Z. Chen, and S. B. Kjaer, "Power electronics as efficient interface in dispersed power generation systems," IEEE Trans. Power Electron., vol. 19, no. 5, pp. 1184–1194, Sep. 2004

[13] Peng, F.Z., Tolbert, L.M. and Khan, F., Power electronics' circuit topology-the basic switching cells. In IEEE Workshop Power Electronics Education, pp. 52-57, 2005.

[14] Wu, T.F., "Decoding and synthesizing transformerless PWM converters" IEEE Transactions on Power Electronics, 31(9), pp.6293-6304, 2015.

[15] S. Athikkal, K. Sundaramoorthy, and A. Sankar, "Development and performance analysis of dual-input DC–DC converters for DC microgrid application," IEEJ Trans. Electr. Electron. Eng., 13(7), pp. 1034–1043, 2018.

[16] S. Ding, H. Wu, Y. Xing, Y. Fang, and X. Ma, "Topology and control of a family of non-isolated three-port DC-DC converters with a bidirectional cell," Conf. Proc. - IEEE Appl. Power Electron. Conf. Expo. - APEC, pp. 1089–1094, 2013.

[17]] Liu, Y.C. and Chen, Y.M., 2009, "A systematic approach to synthesizing multiinput DC–DC converters," IEEE Transactions on Power Electronics, 24(1), pp.116-127, 2009.

[18] A. Khaligh, J. Cao, and Y. J. Lee, "A multiple-input dc–dc converter topology," IEEE Trans. Power Electron., vol. 24, no. 3, pp. 862-868, Mar. 2009.

[19] D. E. Van, J. N. Spruijt, D. M. O'sullivan, and J. B. Klaassens, " PWM-switch modeling of DC-DC converters," IEEE Trans. Power Electron., vol. 10, no. 6, pp.659- 65, Nov. 1995.

[20] Veerachary M, Tewari VK, Anandh N (2013) Two-input boosting dc-dc converter for dc-grid applications. International conference on green computing, communication and conservation of energy (ICGCE). IEEE, pp 574–579.

[21] M. Veerachary and V. K. Tiwari, "Power management in dc-grid through two-input dc-dc converter," 2014 Eighteenth National Power Systems Conference (NPSC), Guwahati, India, 2014, pp. 1-6, doi: 10.1109/NPSC.2014.7103876.

[22] Tewari, V.K., Verma, A. Two-Loop Controlled Quasi Multiple-Input DC—DC Converter for Load Voltage and Source Current Management. Trans. Electr. Electron. Mater. 23, 72–80 (2022).

[23] Tewari, V.K., Verma, A. Design and Application of Double-Gate MOSFET in Two Loops Controlled Multi-Input DC-DC Converter. Silicon 14, 7321–7333 (2022).